Discovery of dual-acting opioid ligand and TRPV1 antagonists as novel therapeutic agents for pain

Hobin Lee, Songyeon Ahn, Jihyae Ann, Heejin Ha, Young Dong Yoo, Young Ho Kim, Ji-Young Hwang, Kwang-Hyun Hur, Choon-Gon Jang, Larry V. Pearce, Timothy E. Esch, Nancy E. Lewin, Peter M. Blumberg, Jeewoo Lee

PII: S0223-5234(19)30768-8

DOI: https://doi.org/10.1016/j.ejmech.2019.111634

Reference: EJMECH 111634

To appear in: *European Journal of Medicinal Chemistry*

Received Date: 15 April 2019

Revised Date: 19 August 2019

Accepted Date: 19 August 2019

Please cite this article as: H. Lee, S. Ahn, J. Ann, H. Ha, Y.D. Yoo, Y.H. Kim, J.-Y. Hwang, K.-H. Hur, C.-G. Jang, L.V. Pearce, T.E. Esch, N.E. Lewin, P.M. Blumberg, J. Lee, Discovery of dual-acting opioid ligand and TRPV1 antagonists as novel therapeutic agents for pain, *European Journal of Medicinal Chemistry* (2019), doi: https://doi.org/10.1016/j.ejmech.2019.111634.

Graphical Abstract

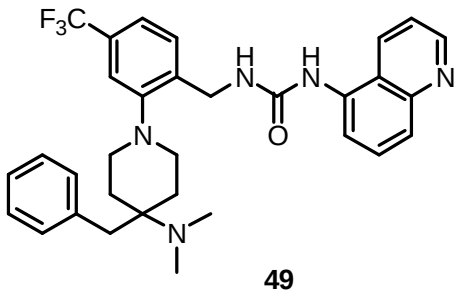

49

TRPV1
binding affinity : K_i = 10.8 nM
antagonism : $K_{i(ant)}$ = 32 nM
MOR
binding affinity : K_i = 29 nM

In vivo formalin test
IC_{50} = 10.5 mg/kg

Discovery of Dual-acting Opioid Ligand and TRPV1 Antagonists as Novel Therapeutic Agents for Pain

Hobin Lee [a], Songyeon Ahn [a], Jihyae Ann [a], Heejin Ha [b], Young Dong Yoo [b], Young Ho Kim [b], Ji-Young Hwang [c], Kwang-Hyun Hur [c], Choon-Gon Jang [c], Larry V. Pearce [d], Timothy E. Esch [d], Nancy E. Lewin [d], Peter M. Blumberg [d], Jeewoo Lee [a,*]

[a] Laboratory of Medicinal Chemistry, College of Pharmacy, Seoul National University, Seoul 08826, Korea

[b] Medifron DBT, Sandanro 349, Danwon-Gu, Ansan-City, Gyeonggi-Do 15426, Republic of Korea

[c] Department of Pharmacology, School of Pharmacy, Sungkyunkwan University, Suwon, Gyeonggi-do 16419, South Korea

[d] Laboratory of Cancer Biology and Genetics, Center for Cancer Research, National Cancer Institute, NIH, Bethesda, MD 20892-4255, USA

* To whom correspondence should be addressed.
Phone: 82-2-880-7846
Fax: 82-2-883-9172
E-mail: jeewoo@snu.ac.kr

Key Words: TRPV1; mu-opioid receptor; analgesic; dual-acting mechanism

Abstract

In order to discover a novel type of analgesic, we investigated dual activity ligands with TRPV1 antagonism and mu-opioid receptor affinity with the goal of eliciting synergistic analgesia while avoiding the side effects associated with single targeting. Based on a combination approach, a series of 4-benzyl-4-(dimethylamino)piperidinyl analogues were designed, synthesized and evaluated for their receptor activities. Among them, compound **49** exhibited the most promising dual-acting activity toward TRPV1 and the mu-opioid receptor *in vitro*. *In vivo,* **49** displayed potent, dose-dependent antinociceptive activity in both the 1^{st} and 2^{nd} phases in the formalin assay. Consistent with its postulated mechanism, we confirmed that *in vivo*, as *in vitro*, compound **49** both antagonized TRPV1 and functioned as a mu-opioid agonist. This result indicates that dual-acting TRPV1 antagonist / mu-opioid ligands can be made and represent a new and promising class of analgesic.

1. Introduction

Pain results from a complex interaction between specialized nerves and signalling systems. Since the transmission of pain signals involves a multitude of parallel processes, a single-target analgesic may not be as effective as would be suggested by the agent's high selectivity and potency. An alternative approach is to seek simultaneous intervention at multiple nodes in these parallel pathways through a single multi-target drug. There is now abundant validation of this multi-target drug strategy showing the integration of simultaneous actions on multiple targets.[1] A further benefit of this approach is that the relatively lower affinity of multi-target agents may not only elicit a synergistic therapeutic effect by the the combination of various mechanistic actions but also show reduced side effects.

Most strong pain-relieving analgesics currently in use act through the opioid receptor. The opioid receptor has four subtypes, the mu, delta, kappa and nociceptin receptors.[2] Among them, mu-opioid receptor (MOR) agonists are the most commonly used opioids for pain management. MOR is an inhibitory G-coupled protein receptor found presynaptically and postsynaptically on various nerve fibers in both the brainstem and spinal cord. Binding of an agonist to the receptor leads to a reduction in cAMP, decreasing intracellular Ca^{2+} levels and inhibiting release of the nerve fiber's neurotransmitters. The other effect of MOR activation is an increase in potassium efflux out of the nerve fiber causing hyperpolarization of the nerve.

The transient receptor potential vanilloid 1 (TRPV1) has emerged as a promising therapeutic target for the treatment of neuropathic pain and a range of other conditions, reflecting the central role of this nociceptor in the function of C-fiber sensory neurons.[3] The receptor functions as a non-selective cation channel with high Ca^{2+} permeability. Different classes of activators, such as low pH, noxious heat, endogenous lipid mediators and natural vanilloids, cause an increase in intracellular Ca^{2+}, thereby resulting in the excitation of the primary sensory neurons and the consequent central perception. Therefore, TRPV1 antagonists inhibit this transmission of

nociceptive signaling from the periphery to the CNS, providing therapeutic potential for novel analgesic and antiinflammatory agents.[4]

In order to discover novel analgesics with a multi-target mechanism, we investigated new dual-target compounds acting both as a MOR ligand and a TRPV1 antagonist. This type of compound should not only block pain transmission in both the peripheral and central nervous system but may also reduce the side effects associated with single targeting, such as reinforcement disorders, nausea, drowsiness and respiratory depression from mu-receptor agonism and marked hyperthermia and impaired noxious heat sensation from TRPV1 antagonism.

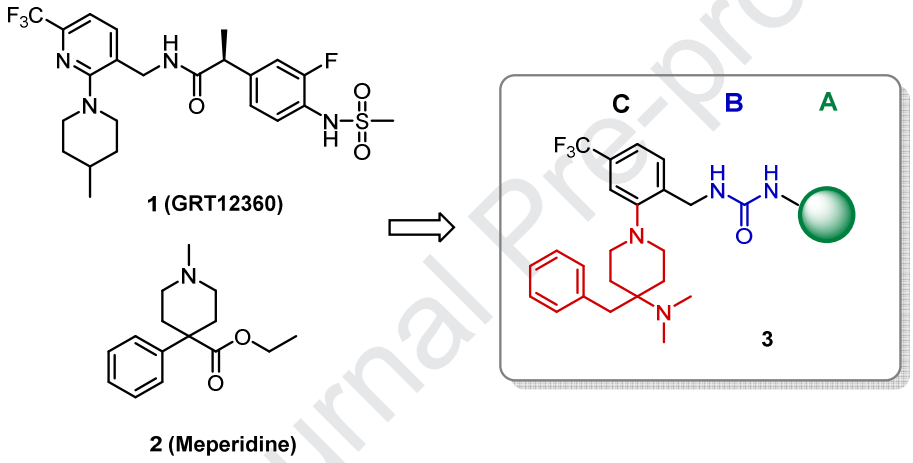

Figure 1. Design of novel dual-acting scaffold

In order to design a dual-acting scaffold, we combined the key pharmacophores of the potent TRPV1 antagonist **1** (**GRT12360**)[5] and the piperidine MOR agonist **2** (**Meperidine**) to generate a hydrid **3** (**Figure 1**). In this design, the 4-methylpiperidinyl moiety in **1** was replaced with the structurally similar 4-benzyl-4-(dimethylamino)piperidinyl (BDP) group that was known as a novel synthetic opioid (NSO)[6]. In addition, the pyridine and propanamide groups of **1** were switched with the synthetically more accessible phenyl and urea surrogates, respectively. In this new scaffold **3**, a variety of substituted phenyl and heterocycles present in potent TRPV1 antagonists previously reported were incorporated into the A-region. The synthesized compounds

were assayed *in vitro* for MOR binding affinity and TRPV1 receptor activity. Then, the most promising selected dual-acting compound in the series was tested in the formalin model to evaluate its *in vivo* antinociceptive activity. Finally, it was confirmed that this compound indeed targeted the mu-opioid receptor and TRPV1 *in vivo*, as it did *in vitro*.

2. Results and discussion

2.1. Chemistry

The C-region amine **8** was synthesized from commercially available 1-(*tert*-butoxy carbonyl)-4-piperidone **4** in 5 steps (**Scheme 1**). The 4-keto group of **4** was converted to the 4-cyano-4-dimethylamino moiety by the Strecker reaction in which the cyano group was substituted with a benzyl group by Grignard reagent to afford **6**. The piperidine **6** was reacted with 2-fluoro-4-(trifluoromethyl)benzonitrile under basic conditions to give *N*-aryl piperidine **7**. The nitrile of **7** was reduced to the corresponding amine **8** which was converted to phenyl carbamate **9**. Either amine **8** or carbamate **9** was used for the coupling reaction with the corresponding A-region carbamate or amine, respectively, to provide the final compounds.

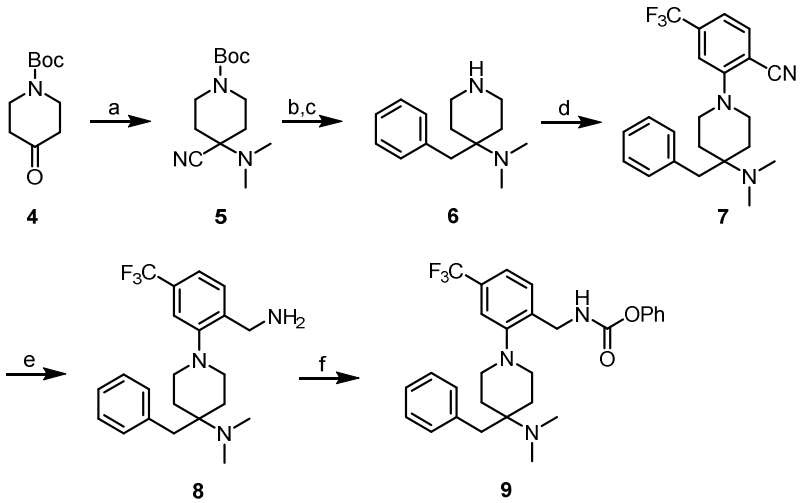

Scheme 1. Synthesis of the C-region.

Reagent and Conditions: (a) dimethylamine, KCN, MeOH, H_2O, 0 ^oC to r.t, 24 h, 99%; (b) BnMgCl, THF, reflux, 3 h, 55%; (c) CF_3CO_2H, CH_2Cl_2, r.t, 1 h, 95%; (d) 2-fluoro-4-(trifluoromethyl)benzonitrile, K_2CO_3, 18-crown-6-ether, MeCN, reflux, overnight, 37%; (e) $BH_2{\cdot}SMe_2$, THF, reflux, overnight, 11%; (f) phenyl chloroformate, THF, MeCN, pyridine, 0 ^oC to r.t, 1 h, 99%.

For the synthesis of 4-methylsulfonamidophenyl A-region analogues (**Scheme 2**), the propionic acid **10**[5] was coupled with the C-region amine **8** under EDC conditions to give the propanamide **11**. The phenyl carbamates, **12** and **14**,[7] were condensed with amine **8** to provide the ureas **13** and **15** as one-carbon elongated A-region analogues. The benzylamine **16**[7] was reacted with carbamate **9** to give the urea **17** as a one-carbon elongated B-region analogue.

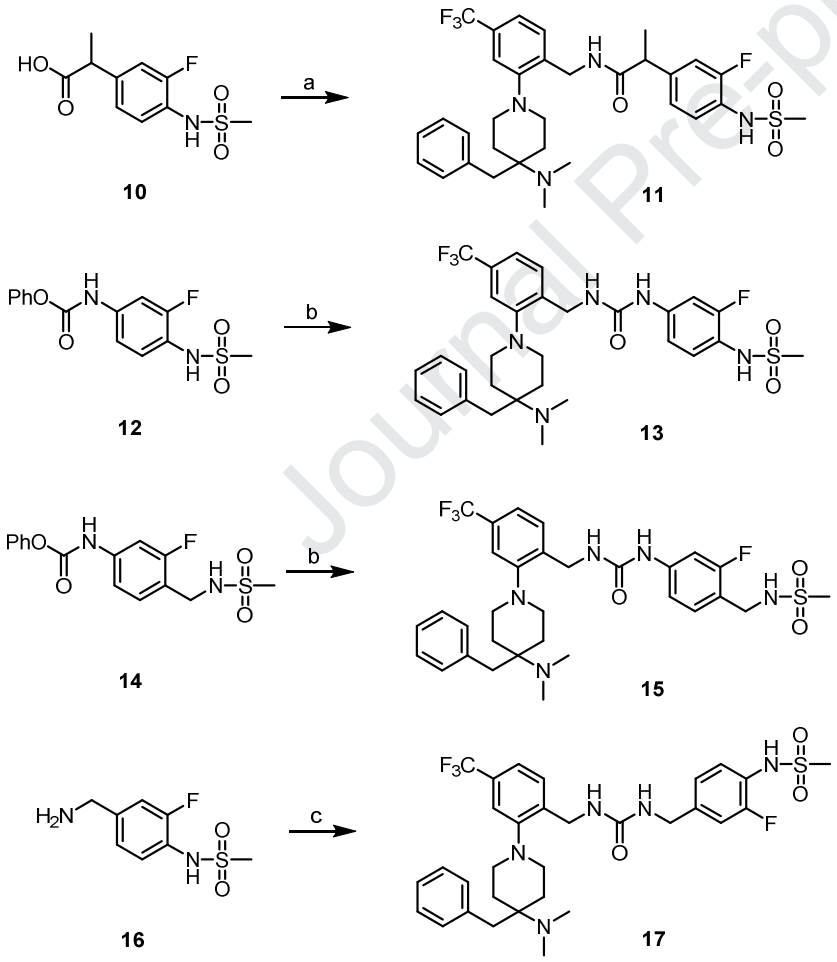

Scheme 2. Synthesis of 3-fluoro-4-methylsulfonamidophenyl A-region analogues
Reagent and conditions: (a) amine **8**, HOBt, EDC, TEA, 1,4-dioxane, r.t, overnight, 42%; (b) amine **8**, DMAP, MeCN, 50 ^oC, overnight, 41-45%; (c) carbamate **9**, DBU, DMF, 100 ^oC, overnight, 34%.

As the A-region bioisosteres of **15**, its sulfamoylamino and hydroxyl surrogates were synthesized (**Scheme 3**). Starting from 2-fluoro-4-nitrobenzyl amine **18**, the amine was converted to the *N*-Boc sulfamoylamino group using chlorosulfonyl isocyanate and *t*-butanol and then the 4-nitro group was transformed to the phenylcarbamate **19**. For the synthesis of the hydroxyl analogue, 2-fluoro-4-nitrobenzoic acid **21** was reduced to the corresponding alcohol and then the 4-nitro group was converted to the phenylcarbamate **22**. The condensation of **19** and **22** with amine **8** provided the final sulfamoylamino and hydroxyl analogues, **20** and **23**, respectively.

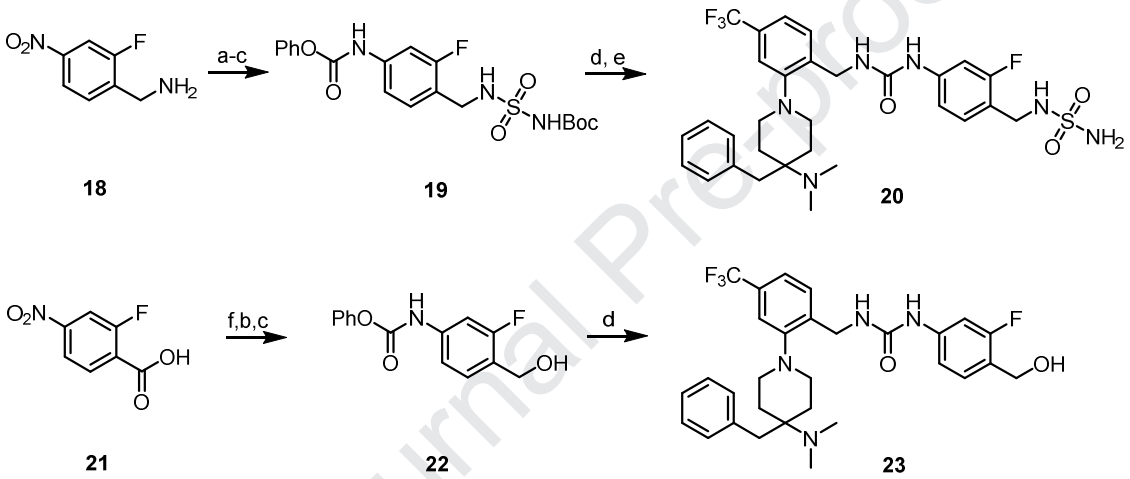

Scheme 3. Synthesis of (4-sulfamoylamino)methyl and 4-hydroxymethyl A-region analogues
Reagent and conditions: (a) $ClSO_2$-N=C=O , t-BuOH, CH_2Cl_2, TEA, 0 ^oC to r.t., 75%; (b) 10% Pd/C, H_2, THF-EtOH (1:1), r.t ., 3 h, 95%; (c) phenyl chloroformate, pyridine, THF, MeCN, r.t., 1 h, 90%; (d) amine **8**, DMAP, MeCN, 50 ^oC, overnight, 55-63%; (e) CF_3CO_2H, CH_2Cl_2, r.t, 1 h, 64%; (f) $LiAlH_4$, Et_2O, reflux, 30 min, 55%.

For the synthesis of 7-hydroxynaphthalen A-region analogues (**Scheme 4**), commercially available 8-aminonaphthalen-2-ol **24** was converted to the corresponding phenylcarbamate **25** or reduced and then carbamoylated to the tetrahydronaphthalene **27**. The condensation of **25** and **27** with amine **8** provided the final products, **26** and **28**, respectively.

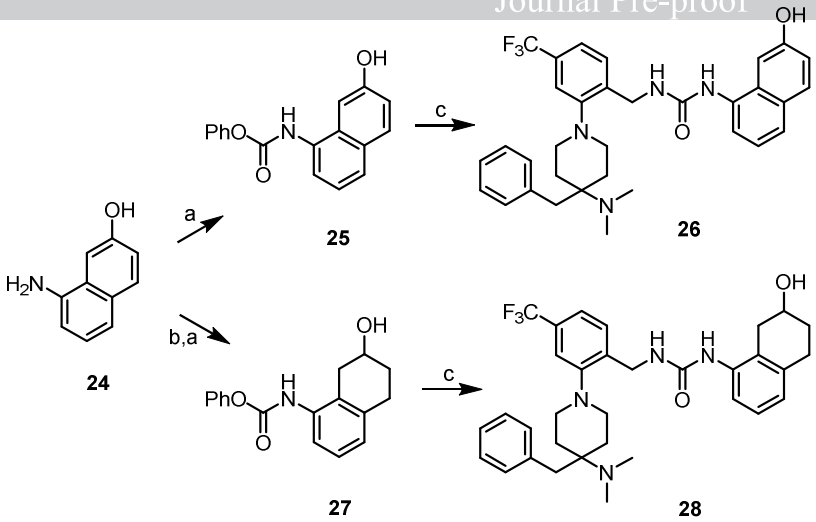

Scheme 4. Synthesis of 7-hydroxynaphthalen A-region analogues
Reagent and conditions: (a) pyridine, phenyl chloroformate, acetone, 0 ^{o}C to r.t, 30 min, 70-85%; (b) 2N HCl in 1,4-dioxane, PtO_2, H_2, ethanol, 45 ^{o}C, overnight, 65%; (c) amine **8**, DMAP, MeCN, 50 ^{o}C, overnight, 59-60%.

For the synthesis of dihydrobenzofuran A-region analogue (**Scheme 5**), 2,3-dihydrobenzofuran **29** was converted to the desired 6-nitro-2,3-dihydrobenzofuran **31** in 6 steps. The nitro group of **31** was tranformed to the corresponding phenyl carbamate **32** which was condensed with amine **8** to afford the final compound **33**.

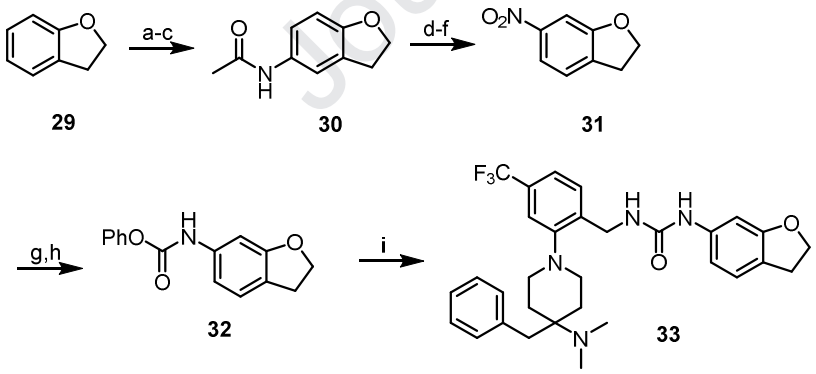

Scheme 5. **Synthesis of the 2,3-dihydrobenzofuran A-region analogue.**
Reagent and conditions: (a) acetyl chloride, $AgNO_3$, MeCN, 0 ^{o}C, 1 h, 35%; (b) 10 % Pd/C, H_2, MeOH, THF, r.t., overnight, 82%; (c) acetic anhydride, 1,4-dioxane, r.t, overnight, 86%; (d) HNO_3, acetic acid, r.t, overnight, 28%; (e) c.HCl, ethanol, reflux, 2 h, 65%; (f) isoamylnitrite, THF, reflux, 41%; (g) 10 % Pd/C, H_2, MeOH, r.t., overnight, 75%; (h) phenyl chloroformate, THF, MeCN, pyridine, 0 ^{o}C to r.t., 1 h, 87%; (i) amine **8**, DMAP, MeCN, 50 ^{o}C, overnight, 30%.

For the synthesis of quinolinone and isoquinolinone analogues (**Scheme 6**), the 5-aminoquinolin-2-one **34** and 5-aminoisoquinolin-1-one **36** previously reported[8] were converted the corresponding phenyl carbamates and then coupled with the amine **8** to provide the quinolin-2-one **35** and isoquinolin-1-one **37**, respectively.

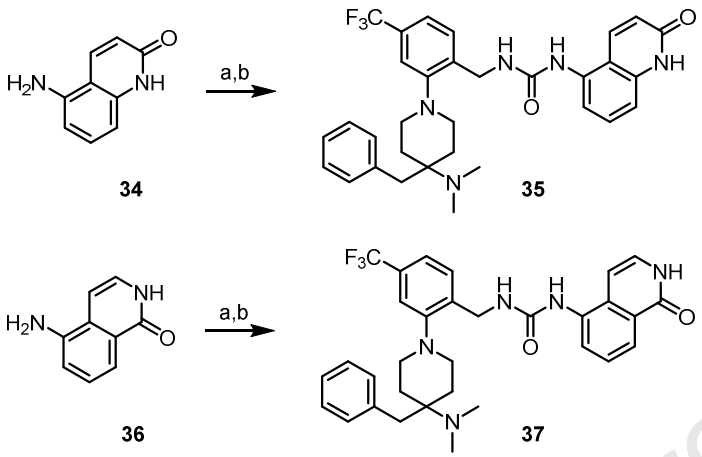

Scheme 6. Synthesis of the quinolinone A-region analogues.
Reagent and conditions: (a) phenyl chloroformate, THF, MeCN, Pyridine, 0 ^{o}C to r.t., 1 h, 80-86%; (b) amine **8**, DMAP, MeCN, 50 ^{o}C, overnight, 30-40%.

Finally, for the synthesis of quinoline and isoquinoline analogues (**Scheme 7**), aminoquinolines and aminoisoquinolines (**38**-**43**), which were commercially available or previously reported[9], were converted to the corresponding phenyl carbamate or trichloroacetamide, which were reacted with the amine **8** to provide the final compounds (**44**-**49**), respectively.

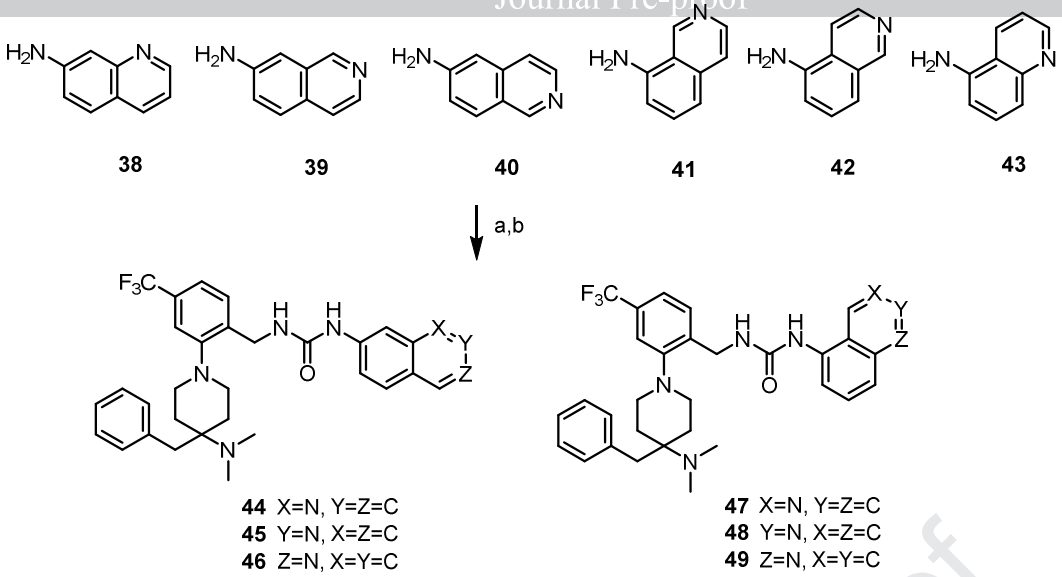

Scheme 7. Synthesis of the quinoline A-region analogues.
Reagent and conditions: (a) [Method A] phenyl chloroformate, pyridine, THF, MeCN, 0 ^{o}C to r.t, 2 h for **44, 45, 47, 48, 49**, 60-75% [Method B] Trichloroacetyl chloride, TEA, CH_2Cl_2 for **46**, 63%; (b) [Method A] amine **8**, DMAP, MeCN, 50 ^{o}C, overnight for **44, 45, 47, 48, 49**, F [Method B] amine **8**, DBU, MeCN, reflux, overnight for **46**, 25%.

2.2. *In vitro* activity

The binding affinities and potencies as TRPV1 agonists/antagonists of dual-acting ligands were assessed *in vitro* by a binding competition assay with [^{3}H]resiniferatoxin (RTX) and by a functional $^{45}Ca^{2+}$ uptake assay using human TRPV1 heterologously expressed in Chinese hamster ovary (CHO) cells, as previously described.[10] For the agonism assay, a saturating concentration of capsaicin (1 μM) was used to define maximal response. For the antagonism assay, the dose-dependent inhibition of the capsaicin (30 nM) stimulated calcium uptake was measured. The K_i values for antagonism take into account the competition between capsaicin and the antagonist. The binding affinities as mu opioid ligands were measured by a binding competition assay with [^{3}H]-D-Ala^2-MePhe^4-Glyol^5-enkephalin (DAMGO).[11,12] The K_i values was calculated from the measured IC_{50} values using the Cheng-Prusoff equation.[13] The results are shown in **Table 1** together with those for morphine (K_i = 6.08 nM) and **1** ($K_{i(ant)}$ = 2.22 nM) as references.

First, we investigated 4-methylsulfonamidophenyl A-region analogues. The direct substitution of the 4-methylpiperidinyl group in **1** with the BDP group, providing **11**, showed

similar activity in the binding affinity and antagonism toward TRPV1 compared to **1**. However, its binding affinity to MOR decreased significantly compared to that of morphine. The urea B-region analogues of **11** (**13**, **15**, **17**) were next examined. Compound **13**, the urea surrogate of **11**, displayed weak activity on both TRPV1 and MOR. On the other hand, whereas compound **15**, the one-carbon elongated analogue in the A-region, exhibited improved TRPV1 antagonism, compound **17**, the one-carbon elongated analogue in the B-region, displayed enhanced MOR activity. However, neither compound showed the desired dual-acting activity. The sulfamide analogue **20** showed improved MOR activity comparable to **17**, but reduced TRPV1 antagonism compared to **15**. The 4-hydroxymethyl analogue **23** did not displayed any substantial improvement in either receptor activity compared to **15**.

Next, we investigated the bicyclic A-region analogues. Previously, the 7-hydroxynaphthalen-1-yl[14] and 7-hydroxytetrahydronaphthalen-1-yl[15] urea analogues showed potent TRPV1 antagonism. Based on that fact, we examined their BDP C-region analogues, **26** and **28**. Both showed high affinity and potent TRPV1 antagonism; however, their MOR activity was modest. In addition, the 2,3-dihydrobenofuran-6-yl urea analogue **33** was examined, but the receptor activities were also moderate. Recently, we discovered two distinct A-regions for TRPV1 functional activity, quinolin-2-one-5-yl (**34**) and isoquinolin-1-one-5-yl (**35**), where derivatives of **34** displayed potent antagonism and derivatives of **36** displayed potent agonism, regardless of the C-region.[8] Similarly, their BDP C-region analogues (**35**, **37**) displayed the same functional activities, respectively, however the potencies in TRPV1 and MOR were moderate.

Finally, we explored quinoline and isoquinoline A-region analogues. Previously, we reported that 6,6-fused heterocyclic ureas displayed highly potent TRPV1 antagonism.[9] Based on that, we investigated their BDP C-region analogues including quinolin-7-yl (**44**), isoquinolin-7-yl (**45**), isoquinolin-6-yl (**46**), isoquinolin-8-yl (**47**), isoquinolin-5-yl (**48**) and quinolin-5-yl (**49**) derivatives.

Whereas the β-substituted ring analogues (**44**-**46**) exhibited moderate TRPV1 antagonism, the α-substituted ring analogues (**47**-**49**) displayed potent TRPV1 antagonism. Among them, compounds **46** and **49** showed reasonable MOR activities with K_i = 17 and 29 nM, respectively, that were just 3- and 5-fold less potent than that of morphine. Considering the two receptor activity, compound **49** was selected as most promising candidate with a dual-acting mechanism.

Table 1. *In vitro* activity of 4-benzyl-4-(dimethylamino)piperidinyl derivatives on *h*TRPV1 and MOR

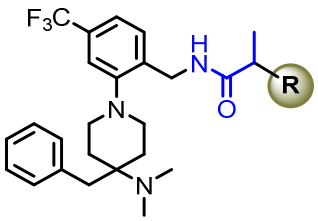

11

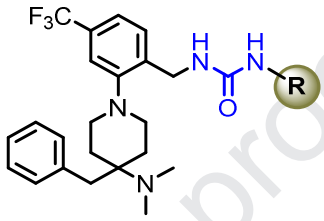

13-49

	R	TRPV1[a]			MOR
		Binding Affinity K_i (nM)	**Agonism EC_{50} (nM)**	**Antagonism $K_{i(ant)}$ (nM)**	**Binding Affinity K_i (nM)**
Morphine					6.08
1 (rac)		7.9 (±1.6)	NE	2.22 (±0.47)	
11	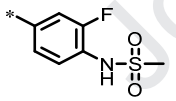	3.79 (±0.19)	NE	8.2 (±1.7)	428
13	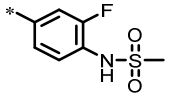	1159 (±35)	NE	WE	368
15	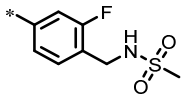	16.4 (±0.90)	NE	25.0 (±1.4)	322
17	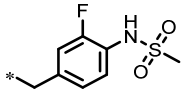	266 (±69)	NE	85.9 (±7.0)	76.2
20	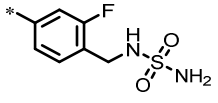	15.3 (±3.6)	NE	120 (±19)	72.4

23	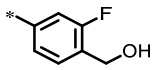	27.9 (±7.6)	NE	81 (±19)	240
26	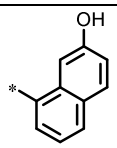	0.46 (±0.07)	NE	8.9 (±1.2)	137
28	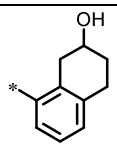	0.95 (±0.20)	NE	10.1 (±0.78)	261
33	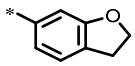	41.4 (±8.1)	NE	31.3 (±9.5)	225
35	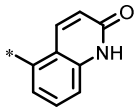	1.67 (±0.50)	NE	30.6 (±3.8)	240
37	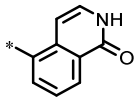	111 (±15)	43.7 (±6.7)	NE	105
44	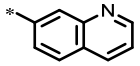	14.1 (±2.9)	NE	42 (±14)	166
45	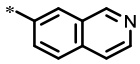	7.33 (±0.26)	NE	56.1 (±7.2)	177
46	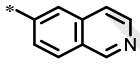	62 (±10)	NE	156 (±50)	17.0
47	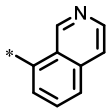	12.3 (±4.3)	NE	18.68 (±1.2)	205
48	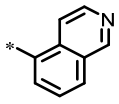	0.67 (±0.13)	NE	8.8 (±4.1)	507
49	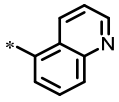	10.8 (±1.6)	NE	32 (±14)	29

[a] NE: no effect, WE: weak effect; values for TRPV1 are the mean of at least three experiments; values for MOR represent single experiments.

2.3. *In vivo* activity

In order to evaluate antinociceptive activity of compound **49**, we conducted the formalin assay in ICR mice.[16,17] In this assay, the compound was administered by intraperitoneal (i.p.) injection 30 min before subcutaneous (s.c.) injection of 2% formalin solution into the hindpaw and then the pain response of licking and biting of the injected paw was evaluated over the next 30 min. The evaluation was performed over two discrete phases (1st phase, 0-5 min; 2nd phase, 20-30 min) of the response upon formalin injection. The 1st Phase (0-5 min) models acute pain, whereas the 2nd phase (20-30 min) models chronic pain. As shown in **Figure 2**, compound **49** exhibited potent antinociceptive activity in a dose-response fashion with an ED_{50} of 23.9 mg/kg in the 1st phase and 10.5 mg/kg in the 2nd phase, respectively. In addition, at a dose of 40 mg/kg compound **49** was able to inhibit the pain behavior completely in phase 2.

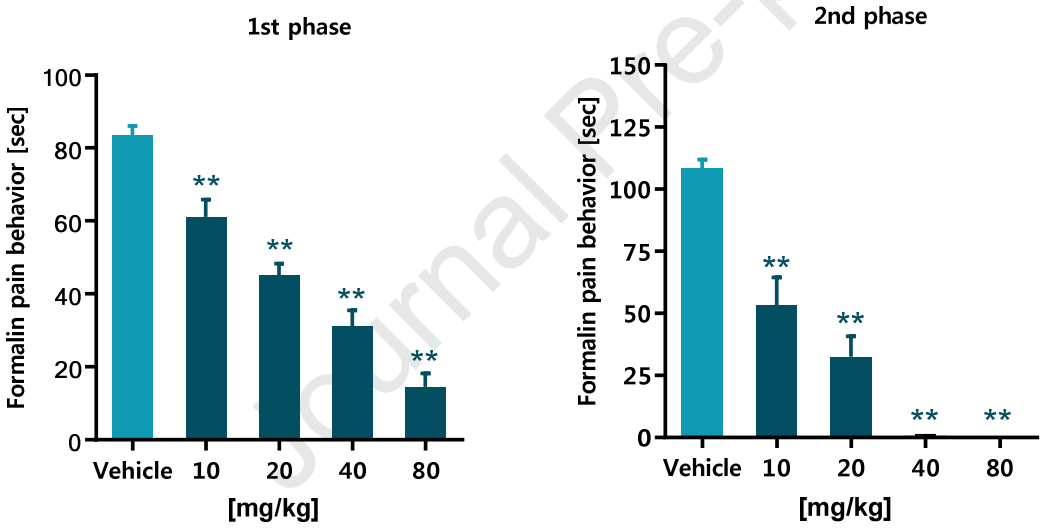

Figure 2. Antinociceptive activity of compound **49** in formalin assay

2.4. Target engagement study

To determine whether the antinociceptive effect of compound **49** was derived from *in vivo* MOR activation and TRPV1 antagonism, we confirmed the target engagement of **49** employing the capsaicin-induced paw licking model[18] and a MOR antagonist pain model[19].

The involvement of TRPV1 in the antinociceptive activity of **49** was investigated using the capsaicin-induced paw licking model as a model of pain induced by capsaicin. As shown in **Figure**

3A, compound **49** administered intraperitoneally showed a dose-dependent reduction in the capsaicin-induced nociceptive response, producing 64.8 and 89.6% inhibition against capsaicin-induced pain compared to vehicle at doses of 20 and 40 mg/kg, respectively. These results confirm that capsaicin-induced pain, which is mediated through TRPV1, was antagonized *in vivo* by **49**.

The involvement of MOR in the antinociceptive activity of **49** was investigated using naloxone, a MOR antagonist, in the formalin model. As shown in **Figure 3B**, intraperitoneal administration of compound **49** decreased the paw licking time by 52.5 and 90.2 % in the 1st and 2nd phases at a dose of 30 mg/kg, respectively. However, following pretreatment with naloxone (10 mg/kg, i.p.), the licking time in response to compound **49** was reduced to 5.7 and 47.9 % in 1st and 2nd phases, respectively, indicating that the analgesic effect of **49** was significantly reversed by naloxone in both phases of the formalin-induced nociception.

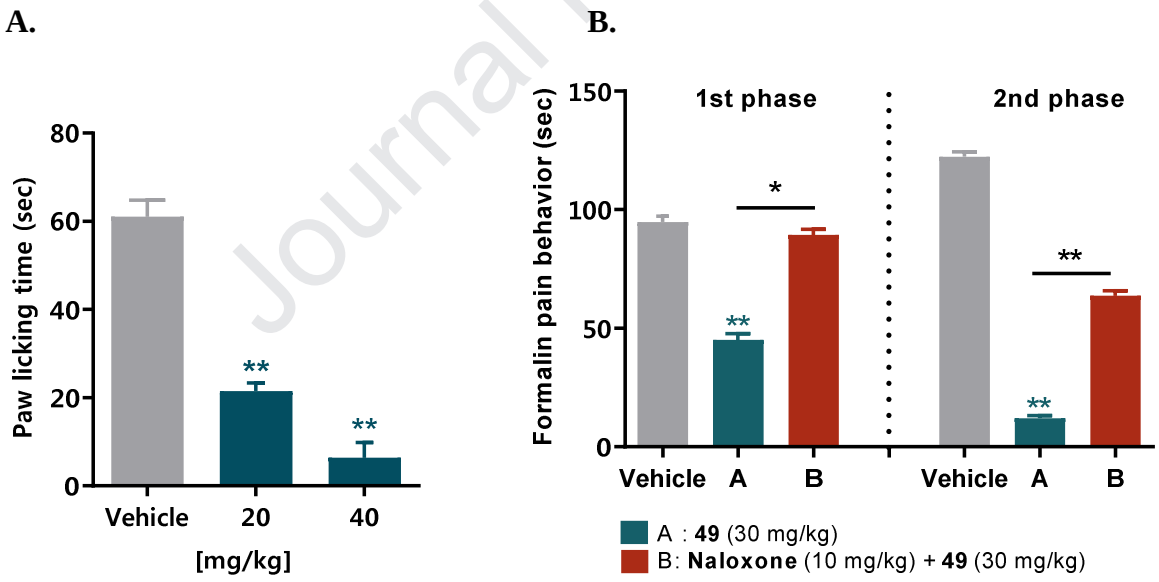

Figure 3. (A) Compound **49** blocks capsaicin-induced licking behavior in mice. Results are expressed as mean ± SEM (n = 3-4). **p<0.01 compared to vehicle-treated group. (B) Pretreatment of naloxone significantly inhibits the analgesic effect of compound **49** in the formalin test. Results are expressed as mean ± SEM (n=3-4). *p<0.05; **p<0.01 compared with vehicle-treated group: **p<0.01 compared with **49** group.

3. Conclusion

In order to discover a novel analgesic with a multi-target mechanism, we investigated dual-acting compounds with MOR ligand and TRPV1 antagonist activities. This type of compound could potentially not only block the pain transmission in both the peripheral and central nervous system but also minimize the side effects associated with single targeting. For the design of dual-acting compounds, we combined the 4-benzyl-4-(dimethylamino)piperidinyl group known as NSO with a potent TRPV1 antagonist template to generate a new scaffold in which the A-region was variably modified with substituted aryl groups, including 3-fluoro-4-methylsulfonamidophenyl analogues, (tetrahydro)naphthalene, and 6,6-fused heterocycles used as the A-region in previous potent TRPV1 antagonists. Among them, compound **49** displayed the most promising dual-acting activity with $K_{i(ant)}$ = 32 nM for TRPV1 and K_i = 29 nM for MOR. An *in vivo* study of compound **49** in the formalin test indicated that **49** showed potent and dose-dependent antinociceptive activity with ED_{50} = 23.9 and 10.5 mg/kg in 1st and 2nd phases, respectively. The target engagement study indicated that capsaicin-induced nociception was significantly reduced by **49** and the antinociceptive effect of **49** in the formalin model was blocked by the pretreatment of naloxone, suggesting that the antinociceptive effect of **49** was derived from both TRPV1 antagonism and MOR activation. The discovery of a new dual-acting compound with activity as a TRPV1 antagonist and as a MOR ligand presents a new direction for the development of novel analgesics to overcome the problems associated with single targeting.

4. Experimental

4.1. Chemistry

All chemical reagents were commercially available. Silica gel column chromatography was performed on silica gel 60, 230-400 mesh, Merck. Nuclear magnetic resonance (^{1}H NMR) spectra were recorded on a JEOL JNM-LA 300 and a Bruker Avance 400 MHz FTNMR spectrometer.

Chemical shifts are reported in ppm units with Me_4Si as a reference standard. Mass spectra were recorded on a VG Trio-2 GC-MS and a 6460 Triple Quad LC/MS.

4.1.1. Synthesis of the C-region

4.1.1.1. tert-Butyl 4-cyano-4-(dimethylamino)piperidine-1-carboxylate (5)

To a solution of **4** (1.0 mmol) in MeOH was added dimethylamine solution (7.0 mmol) and dimethylamine hydrochloride (3.0 mmol). Conc. HCl (0.5 mmol) was then added to the reaction mixture dropwise at 0 ^{o}C over 10 min and the mixture stirred for 1 h at room temperature. Potassium cyanide (3.0 mmol) was added in portions to the reaction mixture and stirred 24 h at room temperature. After completion, the reaction mixture was diluted with water and extracted with EtOAc several times. The combined organic layer was washed with brine, dried over $MgSO_4$, filtered and concentrated *in vacuo*. The residue was purified by silica gel column chromatography to afford ***5*** as a white solid in 99% yield. ^{1}H NMR ($CDCl_3$, 300 MHz) δ 3.97 (d, J = 13.2 Hz, 2H), 3.14 (bt, J = 11.7 Hz, 2H), 2.35 (s, 6H), 2.08 (bd, J = 13.5 Hz, 2H), 1.69-1.59 (m, 2H), 1.46 (s, 9H); FAB-MS *m/z* 254 $[M+H]^+$.

4.1.1.2. 4-Benzyl-N,N-dimethylpiperidin-4-amine (6)

To a solution of **5** (1.0 mmol) in anhydrous THF was added benzylmagnesium chloride (2.0 M in THF, 2.24 mmol). After the reaction mixture was refluxed for 3 h, the reaction mixture was cooled to room temperature, diluted with aq. NH_4Cl and extracted with EtOAc several times. The combined organic layer was washed with brine, dried over $MgSO_4$, filtered and concentrated *in vacuo.* The residue was purified by silica gel column chromatography to afford the desired product. By following the general procedure described in 4.1.2.1, the Boc group was deprotected to give **6** as a white solid in 55% yield. ^{1}H NMR ($CDCl_3$, 400 MHz) δ 7.03 - 7.37 (m, 5H), 3.19 (t, J = 12.2 Hz, 2H), 2.95 (d, J = 12.1 Hz, 2H), 2.66 (s, 2H), 2.25 (s, 6H), 1.88 (d, J = 14.0 Hz, 2H) 1.61 (dd, J = 3.4 Hz, 16.5 Hz, 6H); FAB-MS *m/z* 219 $[M+H]^+$.

4.1.1.3. 2-(4-Benzyl-4-(dimethylamino)piperidin-1-yl)-4-(trifluoromethyl)benzonitrile (7)

To a solution of **6** (1.0 mmol) in CH_3CN, potassium carbonate (2.2 mmol) was added 18-crown-6 ether (0.1 mmol) and 2-fluoro-4-(trifluoromethyl)benzonitrile (0.9 mmol). The reaction mixture was refluxed for 15 h and cooled to room temperature. The mixture was diluted with water and extracted with EtOAc several times. The combined organic layer was washed with brine, dried over $MgSO_4$, filtered and concentrated *in vacuo*. The residue was purified by silica gel column chromatography to afford **7** as a white solid in 37% yield. ^{1}H NMR ($CDCl_3$, 400 MHz) δ 7.55 (d, J = 8.0 Hz, 1H), 7.35 (d, J = 4.6 Hz, 2H), 7.26 (d, J = 7.2 Hz, 1H), 7.07 - 7.21 (m, 4H), 3.21 - 3.33 (m, 4H), 2.71 (s, 2H), 2.33 (s, 6H), 1.93 (dd, J = 2.1, 14.4 Hz, 2H), 1.61 (dd, J = 4.2, 13.5 Hz, 2H); FAB-MS *m/z* 388 $[M+H]^+$.

4.1.1.4. 1-(2-(Aminomethyl)-5-(trifluoromethyl)phenyl)-4-benzyl-N,N-dimethylpiperidin-4-amine (8)

To a solution of **7** (1.0 mmol) in THF, borane dimethylsulfide complex (2 M in THF, 5.0 mmol) was added dropwise and refluxed for 15 h. The mixture was cooled to 0 ^{o}C and quenched by water until the remaining borane was inactivated. The reacton mixture was extracted with CH_2Cl_2 several times. The combined organic layer was washed with brine, dried over $MgSO_4$, filtered and concentrated *in vacuo*. The residue was purified by silica gel colunm chromatography to afford **8** as a pale yellow solid in 11% yield. ^{1}H NMR ($CDCl_3$, 300 MHz) δ 7.45 (s, 1H), 7.29 - 7.34 (m, 3H), 7.16 - 7.23 (m, 4H), 4.73 (*b*s, 2H), 3.92 (t, J = 7.3 Hz, 2H), 3.16 (t, J = 11.2 Hz, 2H), 2.71 - 2.75 (m, 4H), 2.36 (s, 6H), 1.98 (d, J = 12.8 Hz, 2H); FAB-MS *m/z* 392 $[M+H]^+$.

4.1.1.5. Phenyl (2-(4-benzyl-4-(dimethylamino)piperidin-1-yl)-4-(trifluoromethyl)benzyl)carbamate (9)

The title compound was obtained by following the general procedure of **4.1.2.9** as a white solid in 99% yield. ^{1}H NMR ($CDCl_3$, 300 MHz) δ 7.07 - 7.69 (m, 13H), 4.44 (d, J = 5.9 Hz, 2H), 3.31 (t, J

= 11.3 Hz, 2H), 2.73 (m, 4H), 2.36 (s, 6H), 1.92 (d, *J* = 12.5 Hz, 2H), 1.58 (m, 3H); FAB-MS *m/z* 512 $[M+H]^+$.

4.1.2. General procedures

4.1.2.1. Boc deprotection.

To a solution of *N*-Boc protected compound (1.0 mmol) in CH_2Cl_2 was added dropwise trifluoroacetic acid (20 mmol) at 0 °C and stirred for 1 h at room temperature. Then, the reaction mixture was quenched with saturated $NaHCO_3$ solution and extracted with EtOAc several times. The combined organic layer was washed with brine, dried over $MgSO_4$, filtered and concentrated *in vacuo*. The residue was purified by flash column chromatography on silica gel to afford the desired product.

4.1.2.2. N-Boc sulfamide.

Chlorosulfonyl isocyanate (CSI, 1.1 mmol) was dissolved in CH_2Cl_2 and cooled to 0 ^oC. A solution of *tert*-butyl alcohol (1.1 mmol) in CH_2Cl_2 was added dropwise and stirring continued for 30 min at room temperature. The resulting solution was slowly added into a solution of **18** (1.0 mmol) in CH_2Cl_2 and triethylamine (1.1 mmol) at 0 °C. The resulting solution was allowed to warm to room temperature. The reaction mixture was diluted with CH_2Cl_2 and washed with 0.1 N HCl and water. The organic layer was dried over $MgSO_4$, filtered, and concentrated *in vacuo*. The residue was puried by column chromatography on silica gel to afford the desired product.

4.1.2.3. Carboxylic acid reduction.

To a stirred suspension of $LiAlH_4$ (3.0 mmol) in ether was added dropwise a solution of **21** in ether at 0 ^oC over 15 min. The mixture was refluxed for 30 min, then the reaction cooled to 0 ^oC and

quenched with 1N HCl. The precipitate was filtered off and washed with ether. The combined filtrate was dried over $MgSO_4$, filtered and concentrated in *vacuo*. The residue was puried by column chromatography on silica gel to afford the desired product.

4.1.2.4. Catalytic Hydrogenation

Method A. To a solution of nitro compound (1.0 mmol) in MeOH / THF (1:1) was added 10% Pd/C and charged with hydrogen gas. The mixture was stirred for 2 h at room temperature. After completion, the mixture was filtered through celite and the filtrate was concentrated *in vacuo*. The residue was puried by column chromatography on silica gel to afford the desired product.

Method B. To a solution of **24** in EtOH, 2N HCl in 1,4-dioxane and PtO_2 was added and charged with hydrogen gas. The reaction mixture was stirred at 45 ^oC for 15 h. After completion, the mixture was filtered through celite and the filtrate was concentrated *in vacuo*. The compound was used without further purification.

4.1.2.5. Nitration

Method A. A solution of **29** (1.0 mmol) in CH_3CN was cooled to 0 ^oC and was added with silver nitrate (1.0 mmol) and acetyl chloride (1.0 mmol). The reaction mixture was stirred at 0 ^oC for 1 h. After completion, the reaction mixture was diluted with water and extracted with EtOAc several times. The combined organic layer was washed with brine, dried over $MgSO_4$ and concentrated *in vacuo*. The residue was purified by silica gel column chromatography to afford the desire product.

Method B. To a mixture of acetic acid and nitric acid (1.4 mmol) was added dropwise a solution of **30** (1.0 mmol) in acetic acid at 0 ^oC and stirred at room temperture for 15 h. After completion, ice was added to the reaction mixture and the participate was filtered and washed with water several times. The filtrate was dried over $MgSO_4$, concentrated *in vacuo* and the combined solid was used for the next step without further purification.

4.1.2.6. N-Acetylation

To a solution of the appropriate amine (1.0 mmol) in 1,4-dioxane was added acetic anhydride (2.1 mmol) and the mixture was stirred at room temperature for 15 h. After completion, the solution was diluted with water and extrated with EtOAc several times. The combined organic layer was washed with brine, dried over $MgSO_4$, filtered and concentrated *in vacuo*. The residue was purified by silica gel column chromatography to afford the desired product.

4.1.2.7. Deacetylation

A suspension of *N*-acetyl compound (2.07 mmol) and conc. HCl (6.5 mL) in EtOH was refluxed for 2 h. The resulting solution was concentrated under a reduced pressure and carefully neutralized with NH_4OH solution to pH 8. The reaction mixture was extracted with EtOAc, dried over $MgSO_4$, filtered and concentrated *in vacuo*. The residue was purified by silica gel column chromatography to afford the desired product.

4.1.2.8. Deamination

To a solution of the appropriate aryl amine (1.0 mmol) in THF was added isoamylnitrile (3.0 mmol) and the mixture was refluxed for 3 h. After completion, the reaction mixture was cooled to room temperature and diluted with water and extracted with EtOAc several times. The combined organic layer was dried over $MgSO_4$, filtered and concentrated *in vacuo*. The residue was purified by silica gel column chromatography to afford the desired product.

4.1.2.9. Carbamation

To a solution of the appropriate amine (1.0 mmol) in THF was added pyridine (1.1 mmol) and phenyl chloroformate (1.0 mmol) at 0 ^{o}C and stirred at room temperature for 1 h. The reaction mixture was quenched with water and extracted with EtOAc several times. The combined organic layer was washed with brine, dried with $MgSO_4$, filtered and concentrated *in vacuo*. The residue

was purified by silica gel columm chormatography to afford the desired product.

4.1.2.10. Trichloroacetamide

To a solution of the appropriate amine (1.0 mmol) in CH_2Cl_2 was added triethylamine (1.0 mmol) and trichloroacetyl chloride (1.1 mmol) at 0 ^oC and stirred at room temperature for 15 h. After completion, the reaction mixture was diluted with water and extracted with EtOAc several times. The combined organic layer was washed with brine, dried over $MgSO_4$, filtered and concentrated *in vacuo*. The residue was purified by silica gel column chromatography to afford the desired product.

4.1.2.11. Urea coupling

Method A. To a solution of the appropriate carbamate (1.0 mmol) in CH_3CN was added amine (2.0 mmol) and 4-dimethylaminopyridine (1.0 mmol) and stirred at 50 ^oC for 15 h. After completion, the reaction mixture was cooled to room temperature, diluted with water and extracted with EtOAc several times. The combined organic layer was wash with brine, dried with $MgSO_4$, filtered and concentrated *in vacuo*. The residue was purified by silica gel column chromatography (CH_2Cl_2:MeOH=20:1) to afford the desired product in 60-80 % yield.

Method B. To a solution of trichloroacetamide or carbamate (1.0 mmol) in DMF was added the appropriate amine (1.1 mmol) and 1,8-diazabicyclo(5.4.0)undec-7-ene (2.5 mmol). After stirring at 100 ^oC for 15 h, the reaction mixture was cooled to room temperature, diluted with water and extracted with EtOAc several times. The combined organic layer was dried with $MgSO_4$, filtered and concentrated *in vacuo*. The residue was purified by silica gel column chromatography (CH_2Cl_2:MeOH=20:1) to afford the desired product in 70-90% yield.

4.1.2.12. EDC coupling

To a solution of **10** (1.0 mmol) in 1,4-dioxane, **8** (1.05 mmol) was added 1-ethyl-3-(3-dimethylaminopropyl)carbodiimide (1.5 mmol), hydroxybenzotriazole (1.5 mmol) and

triethylamine (2.5 mmol). After stirring at room temperature for 15 h, the reaction mixture was diluted with H_2O and extracted with EtOAc several times. The combined organic layer was washed with brine, dried over $MgSO_4$, filtered and concentrated *in vacuo*. The residue was purified by silica gel column chromatography (CH_2Cl_2:MeOH=20:1) to afford the desired product in 85% yield.

4.1.3. Chemical Spectra

4.1.3.1. N-(2-(4-Benzyl-4-(dimethylamino)piperidin-1-yl)-4-(trifluoromethyl)benzyl)-2-(3-fluoro-4-(methylsulfonamido)phenyl)propanamide (11)

42 % yield, white solid, mp = 80-86 ^oC; ^1H NMR (300 MHz, CD_3OD) δ 6.99-7.35 (m, 11H), 4.25 (s, 2H), 3.54 (m, 1H), 2.96 (d, J = 11.7 Hz, 2H), 2.88 (s, 3H), 2.76 (s, 2H), 2.62 (m, 2H), 2.36 (s, 6H), 1.94 (d, J = 11.0 Hz, 2H), 1.58 (m, 2H), 1.33 (d, J = 7.0 Hz, 3H); HRMS (FAB) calcd for $C_{32}H_{38}F_4N_4O_3S$ $[M + H]^+$ 635.2679, found: 635.2668.

4.1.3.2. N-(4-(3-(2-(4-Benzyl-4-(dimethylamino)piperidin-1-yl)-4-(trifluoromethyl)benzyl)-ureido)-2-fluorophenyl)methanesulfonamide (13)

41 % yield, white solid, mp = 115-120 ^oC; ^1H NMR (300 MHz, DMSO) δ 8.44 (*b*s, 1H), 7.16 - 7.33 (m, 11H), 7.10 (d, J = 8.04 Hz, 2H), 4.15 (d, J = 5.5 Hz, 2H), 2.96 (m, 5H), 2.65 (m, 4H), 2.28 (s, 6H), 1.87 (m, 2H), 1.33 (m, 2H); HRMS (FAB) calcd for $C_{30}H_{35}F_4N_5O_3S$ $[M + H]^+$ 622.2475, found: 622.2476.

4.1.3.3. N-(4-(3-(2-(4-Benzyl-4-(dimethylamino)piperidin-1-yl)-4-(trifluoromethyl)benzyl)-ureido)-2-fluorobenzyl)methanesulfonamide (15)

45 % yield, white solid, mp = 204-207 ^oC; ^1H NMR (300 MHz, DMSO) δ 8.89 (s, 1H), 7.19 - 7.46 (m, 11H), 7.01 (dd, J = 1.8, 8.4 Hz, 1H), 6.66 (t, 1H), 4.21 (d, J = 5.4 Hz, 2H), 4.08 (d, J = 6.0 Hz, 2H), 2.99 (t, J = 11.0 Hz, 2H), 2.84 (s, 3H), 2.70 (m, 4H), 2.30 (s, 6H), 1.92 (d, J = 12.0 Hz, 2H), 1.43 (t, 2H); HRMS (FAB) calcd for $C_{31}H_{37}F_4N_5O_3S$ $[M + H]^+$ 636.2632, found: 636.2625.

4.1.3.4. N-(4-((3-(2-(4-Benzyl-4-(dimethylamino)piperidin-1-yl)-4-(trifluoromethyl)benzyl)-ureido)-methyl)-2-fluorophenyl)methanesulfonamide (17)

34% yield, white solid, mp = 85-90 ^{o}C; ^{1}H NMR (300 MHz, DMSO) δ 9.5 (*b*s, 1H), 7.86 (*b*s, 1H), 7.02 - 7.33 (m, 10H), 6.58 (t, 1H), 6.49 (t, 1H), 4.14 (m, 4H), 2.98 (s, 3H), 2.69 (m, 4 H), 2.29 (s, 6 H), 1.90 (d, *J* = 14.0 Hz, 2H), 1.10 - 1.50 (m, 4H), 0.81 (m, 2 H); HRMS (FAB) calcd for $C_{31}H_{37}F_4N_5O_3S$ $[M + H]^+$ 636.2632, found: 636.2624.

4.1.3.5. N-(4-(3-(2-(4-Benzyl-4-(dimethylamino)piperidin-1-yl)-4-(trifluoromethyl)benzyl)-ureido)-2-fluorobenzyl)aminosulfonamide (20)

64% yield, white solid, mp = 98-101 ^{o}C; ^{1}H NMR (300 MHz, DMSO) δ 8.90 (s, 1H), 7.19 - 7.41 (m, 11H), 6.93 - 7.00 (m, 2H), 6.63 (s, 2H), 4.20 (d, *J* = 5.7 Hz, 2H), 3.99 (d, *J* = 6.2 Hz, 2H), 2.97 (d, *J* = 9.9 Hz, 2H), 2.69 (m, 4H), 2.29 (s, 6H), 1.93 (m, *J* = 10.1 Hz, 2H), 1.43 (*b*s, 2H); HRMS (FAB) calcd for $C_{30}H_{36}F_4N_6O_3S$ $[M + H]^+$ 637.2584, found: 637.2580.

4.1.3.6. 1-(2-(4-Benzyl-4-(dimethylamino)piperidin-1-yl)-4-(trifluoromethyl)benzyl)-3-(3-fluoro-4-(hydroxymethyl)phenyl)urea (23)

55% yield, white solid, mp = 89-94 ^{o}C; ^{1}H NMR (300 MHz, CD_3OD) δ 7.32 - 7.41 (m, 2H), 7.09 - 7.25 (m, 8H), 6.90 (dd, *J* = 1.8, 8.2 Hz, 1H), 4.48 (s, 2H), 4.29 (s, 2H), 3.02 (t, *J* = 11.3 Hz, 2H), 2.69 - 2.77 (m, 4H), 2.37 (s, 6H), 1.92 (d, *J* = 6.2 Hz, 2H), 1.68 (t, *J* = 10.4 Hz, 2H); HRMS (FAB) calcd for $C_{30}H_{34}F_4N_4O_2$ $[M + H]^+$ 559.2696, found: 559.2699.

4.1.3.7. 1-(2-(4-Benzyl-4-(dimethylamino)piperidin-1-yl)-4-(trifluoromethyl)benzyl)-3-(7-hydroxynaphthalen-1-yl)urea (26)

59% yield, light pink solid, mp = 123-127 ^{o}C; ^{1}H NMR (300 MHz, CD_3OD) δ 7.74 (d, *J* = 8.4 Hz, 1H), 7.63 (d, *J* = 8.0 Hz, 1H), 7.07 - 7.48 (m, 12H), 4.37 (s, 2H), 3.03 (t, *J* = 11.3 Hz, 2H), 2.75 (s,

2H), 2.67 (d, *J* = 11.3 Hz, 2H), 2.36 (s, 6H), 1.88 (d, *J* = 13.4 Hz, 2H), 1.53 (t, *J* = 7.1 Hz, 2H); HRMS (FAB) calcd for $C_{33}H_{35}F_3N_4O_2$ $[M + H]^+$ 557.2790, found: 557.2788.

4.1.3.8. 1-(2-(4-Benzyl-4-(dimethylamino)piperidin-1-yl)-4-(trifluoromethyl)benzyl)-3-(7-hydroxy-5,6,7,8-tetrahydronaphthalen-1-yl)urea (28)

60% yield, white solid, mp = 176-179 ^oC; ^1H NMR (300 MHz, $CDCl_3$) δ 7.39 - 7.29 (m, 3H), 6.99 - 7.21 (m, 8H), 6.00 (*b*s, 1H), 5.30 (*b*s, 1H), 4.38 (d, *J* = 3.8 Hz, 2H), 4.11 (m, 1H), 3.05 (t, *J* = 11.2 Hz, 2H), 2.91 - 2.81 (m, 4H), 2.70 (s, 2H), 2.62 (m, 2H), 2.33 (s, 6H), 1.87 (d, *J* = 12.3 Hz, 2H), 1.45 (t, *J* = 11.9 Hz, 2H); HRMS (FAB) calcd for $C_{33}H_{39}F_3N_4O_2$ $[M + H]^+$ 581.3103, found: 581.3102.

4.1.3.9. 1-(2-(4-Benzyl-4-(dimethylamino)piperidin-1-yl)-4-(trifluoromethyl)benzyl)-3-(2,3-dihydrobenzofuran-6-yl)urea (33)

30% yield, white solid, mp = 87-93 ^oC; ^1H NMR (400 MHz, CD_3OD) δ 7.45 (d, *J* = 8.0 Hz, 1H,), 7.40 (s, 1 H), 7.18 - 7.33 (m, 6 H), 7.04 (d, *J* = 8.0 Hz, 1H), 6.88 (d, *J* = 1.7 Hz, 1H), 6.68 (dd, *J* = 1.8, 7.8 Hz, 1H), 4.51 (t, *J* = 8.6 Hz, 2H), 4.37 (s, 2H), 3.08 - 3.13 (m, 4H) 2.88 (s, 2H), 2.83 (m, 2H) 2.48 (s, 6H), 2.01 (m, 2H), 1.75 (m, 2H); HRMS (FAB) calcd for $C_{31}H_{35}F_3N_4O_2$ $[M + H]^+$ 553.2790, found: 553.2787.

4.1.3.10. 1-(2-(4-Benzyl-4-(dimethylamino)piperidin-1-yl)-4-(trifluoromethyl)benzyl)-3-(2-oxo-1,2-dihydroquinolin-5-yl)urea (35)

40% yield, white solid, mp = 125-130 ^oC; ^1H NMR (300 MHz, CD_3OD) δ 7.99 (d, *J* = 8.4 Hz, 1H), 7.12 - 7.51 (m, 11H), 6.57 (d, *J* = 9.9 Hz, 1H), 4.41 (s, 2H), 3.11 (t, *J* = 10.8 Hz, 2H), 2.79 (m, 4H), 2.41 (s, 6H), 1.97 (t, *J* = 14.1 Hz, 2H), 1.65 (t, *J* = 10.6 Hz, 2H); HRMS (FAB) calcd for $C_{32}H_{34}F_3N_5O_2$ $[M + H]^+$ 578.2743, found: 578.2747.

4.1.3.11. 1-(2-(4-Benzyl-4-(dimethylamino)piperidin-1-yl)-4-(trifluoromethyl)benzyl)-3-(1-oxo-1,2-dihydroisoquinolin-5-yl)urea (37)

30% yield, white solid, mp = 104-109 ^{o}C; ^{1}H NMR (400 MHz, CD_3OD) δ 8.14 (d, *J* = 8.1 Hz, 1H), 7.48 (m, 2H), 7.39 (s, 1 H, Ar), 7.33 (d, *J* = 7.8 Hz, 1H), 7.13 - 7.26 (m, 8H), 4.40 (s, 2 H), 3.10 (t, *J* = 10.9 Hz, 2H), 2.78 (s, 2H), 2.73 (d, *J* = 11.4 Hz, 2H), 2.40 (s, 6H), 1.96 (d, *J* = 13.5 Hz, 2H), 1.62 (t, *J* = 11.2 Hz, 2H); HRMS (FAB) calcd for $C_{32}H_{34}F_3N_5O_2$ $[M + H]^+$ 578.2743, found: 578.2747.

4.1.3.12. 1-(2-(4-Benzyl-4-(dimethylamino)piperidin-1-yl)-4-(trifluoromethyl)benzyl)-3-(quinolin-7-yl)urea (44)

46% yield, white solid, mp= 103-106 ^{o}C; ^{1}H NMR (300 MHz, DMSO) δ 9.08 (s, 1H), 8.75 (dd, *J* = 1.8, 4.2 Hz, 1H), 8.19 (d, *J* = 8.2 Hz, 1H), 8.13 (s, 1H), 7.82 (d, *J* = 8.8 Hz, 1H), 7.55 (dd, *J* = 2.0, 8.8 Hz, 1H), 7.45 (d, *J* = 8.1 Hz, 1H), 7.36 (d, *J* = 8.1 Hz, 1H), 7.19 - 7.33 (m, 7H), 6.75 (*b*s, 1 H), 4.26 (d, *J* = 5.5 Hz, 2H), 3.01 (t, *J* = 11.2 Hz, 2H), 2.70 - 2.74 (m, 4H), 2.31 (s, 6H), 1.93 (d, *J* = 18.0 Hz, 2H), 1.45 (*b*s, 2H); HRMS (FAB) calcd for $C_{32}H_{34}F_3N_5O$ $[M + H]^+$ 562.2794, found: 562.2791.

4.1.3.13. 1-(2-(4-Benzyl-4-(dimethylamino)piperidin-1-yl)-4-(trifluoromethyl)benzyl)-3-(isoquinolin-7-yl)urea (45)

51% yield, white solid, mp = 123-127 ^{o}C; ^{1}H NMR (300 MHz, CD_3OD) δ 9.06 (s, 1H), 8.27 (d, *J* = 5.9 Hz, 1H), 8.18 (s, 1H), 7.85 (d, *J* = 9.0 Hz, 1H), 7.70 (m, 2H), 7.49 (d, *J* = 8.0 Hz, 1H), 7.42 (s, 1H), 7.33 (d, *J* = 7.7 Hz, 1H), 7.16 - 7.29 (m, 5H), 4.44 (s, 2H), 3.12 (t, *J* = 10.8 Hz, 2H), 2.85 (m, 4 H), 2.45 (s, 6H), 2.02 (d, *J* = 12.6 Hz, 2H), 1.74 (*b*s, 2H); HRMS (FAB) calcd for $C_{32}H_{34}F_3N_5O$ $[M + H]^+$ 562.2794, found: 562.2799.

4.1.3.14. 1-(2-(4-Benzyl-4-(dimethylamino)piperidin-1-yl)-4-(trifluoromethyl)benzyl)-3-(isoquinolin-6-yl)urea (46)

25% yield, white solid, mp = 99-102 ^{o}C; ^{1}H NMR (400 MHz, CD_3Cl_3) δ 9.06 (s, 1H), 8.38 (d, *J* = 5.8 Hz, 1H), 7.92 (s, 1H), 7.79 (d, *J* = 8.8 Hz, 1H), 7.48 (d, *J* = 5.8 Hz, 1H), 7.26 - 7.42 (m, 5H), 7.06-7.14 (m, 4H), 4.45 (s, 2H), 3.16 (t, *J* = 9.4 Hz, 2H), 2.79 (m, 4H), 2.42 (s, 6H), 2.01 (m, 2H), 1.75 (*b*s, 2H); HRMS (FAB) calcd for $C_{32}H_{34}F_3N_5O$ $[M + H]^+$ 562.2794, found: 562.2800.

4.1.3.15. 1-(2-(4-Benzyl-4-(dimethylamino)piperidin-1-yl)-4-(trifluoromethyl)benzyl)-3-(isoquinolin-8-yl)urea (47)

42% yield, white solid, mp = 144-147 ^{o}C; ^{1}H NMR (300 MHz, $CDCl_3$) δ 9.32 (*b*s, 1H), 8.48 (d, *J* = 5.8 Hz, 1H), 7.60 (m, 4H), 7.34 (d, *J* = 7.9 Hz, 1H) 7.31 (s, 1H), 7.02 - 7.22 (m, 7H), 5.84 (*b*s, 1H), 4.40 (d, *J* = 5.00 Hz, 2H), 3.05 (t, *J* = 10.8 Hz, 2H), 2.65 (m, 4H,), 2.32 (s, 6H), 1.88 (m, 2H), 1.44 (m, 2H); HRMS (FAB) calcd for $C_{32}H_{34}F_3N_5O$ $[M + H]^+$ 562.2794, found: 562.2800.

4.1.3.16. 1-(2-(4-Benzyl-4-(dimethylamino)piperidin-1-yl)-4-(trifluoromethyl)benzyl)-3-(isoquinolin-5-yl)urea (48)

45 % yield, white solid, mp = 106-113 ^{o}C; ^{1}H NMR (300 MHz, CD_3OD) δ 9.12 (s, 1H), 8.32 (d, *J* = 6.03 Hz, 1H), 7.80 (m, 2H), 7.56 (m, 2H), 7.43 (d, *J* = 8.4 Hz, 1H), 7.32 (s, 1H), 7.25 (d, *J* = 7.5 Hz, 1H), 7.04 - 7.14 (m, 5H), 4.45 (s, 2H), 3.01 (t, *J* = 12.5 Hz, 2H), 2.71 (m, 4 H), 2.32 (s, 6H), 1.89 (d, *J* = 14.1 Hz, 2H), 1.57 (*b*s, 2H); HRMS (FAB) calcd for $C_{32}H_{34}F_3N_5O$ $[M + H]^+$ 562.2794, found: 562.2784.

4.1.3.17. 1-(2-(4-Benzyl-4-(dimethylamino)piperidin-1-yl)-4-(trifluoromethyl)benzyl)-3-(quinolin-5-yl)urea (49)

53 % yield, white solid, mp = 183-191 ^{o}C; ^{1}H NMR (300 MHz, DMSO) δ 8.87 (d, *J* = 4.0 Hz, 1H), 8.83 (s, 1 H), 8.48 (d, *J* = 8.6 Hz, 1H), 7.96 (d, *J* = 6.2 Hz, 1H), 7.65 (m, 2H), 7.52 - 7.56 (dd, *J* = 4.02, 8.61 Hz, 1H), 7.48 (d, *J* = 7.9 Hz, 1H), 7.38 (d, *J* = 8.3 Hz, 1H), 7.24 - 7.29 (m, 3H), 7.18 (m, 3H), 6.97 (m, 1H), 4.27 (d, *J* = 5.3 Hz, 2H), 3.00 (t, *J* = 13.6 Hz, 2H), 2.71 (m, 4H), 2.29 (s, 6H),

1.92 (m, 2H), 1.43 (t, J = 11.2 Hz, 2H); HRMS (FAB) calcd for $C_{32}H_{34}F_3N_5O$ $[M + H]^+$ 562.2794, found: 562.2784.

4.2. Biology

4.2.1. TRPV1 assay

4.2.1.1. Cell culture

As previously reported,[10] the selected stable CHO cell line expressing human TRPV1 (Tet-Off system) was cultured in maintaining medium (Ham's F-12 supplemented with 10% fetal bovine serum, 0.025M HEPES pH 7.5, 250 μg/mL Geneticin, and 1mg/L tetracycline). For [^{3}H]RTX competition binding experiments, cells were seeded in 75 cm^2 culture flasks in maintaining media and grown to approximately 90% confluency after 48 h. The flasks were then washed with DPBS (without Ca^{2+} or Mg^{2+}) and the medium was replaced with inducing medium (Ham's F12 supplemented with 10% fetal bovine serum and 0.025 M HEPES pH 7.3) for an additional 48 h. The cells were harvested in Trypsin-EDTA and DPBS (no Ca^{2+} or Mg^{2+}) and pelleted by centrifugation at 1000 rpm for 5 min. The pellets were stored at −20 °C until use.

4.2.1.2. Radioligand binding assay

As previously reported,[10] competition binding studies were performed in the presence of a fixed concentration of [^{3}H]RTX and various concentrations of competing ligands. The binding assay mixtures were handled in borosilicate tubes and contained DPBS (with Ca^{2+} and Mg^{2+}), bovine serum albumin (0.25 mg/mL), [^{3}H]RTX (100 pM), and various concentrations of the ligands for a total volume of 350 μL. Non-specific binding was determined in the presence of non-radioactive RTX (100 nM). The tubes were incubated for 60 min in a 37 °C water bath. The mixtures were then cooled on ice for approximately 10 min, after which bovine glycoprotein fraction VI (100 μL; 2 mg/mL) was added to reduce nonspecific binding. The ice-cold contents were then transferred to

1.5 mL centrifuge tubes for centrifugation. Membrane-bound RTX was separated from free RTX as well as the glycoprotein-bound RTX by pelleting the membranes in a Beckman (Coulter) Allegra 21R centrifuge for 15 min at 12,000 rpm. Radioactivity in the pellets and in an aliquot of each supernatant was determined by scintillation counting in the presence of Cytoscint E.S. (MP Biomedicals). Equilibrium binding parameters (K_i, B_{max}, and cooperativity) were determined by fitting the Hill equation to the measured values.

4.2.1.3. Calcium uptake assay

As previously reported,[10] CHO-hTRPV1 cells were plated in 24-well tissue culture plates with maintaining medium and grown to 50%-70% confluency. The following day, the maintaining medium was aspirated and the cells were washed twice with DPBS (no Ca^{2+} or Mg^{2+}). Inducing medium (without tetracycline) was added and the cells were incubated for an additional 48 h to initiate TRPV1 expression. Experiments were done approximately 48 h after induction. To measure $^{45}Ca^{2+}$ uptake in the assays of agonism, the inducing medium was aspirated and replaced by assay medium (400 μL) in each well. The assay medium consisted of DMEM supplemented with bovine serum albumin (0.25 mg/mL), $^{45}Ca^{2+}$ (37 kBq/mL), and increasing concentrations of the non-radioactive ligand. The cells were incubated for 5 min in a water bath at 37 °C. For a measure of the uptake by a full agonist, a saturating concentration of capsaicin (1 μM) was used. Background uptake was determined in the absence of either compound or capsaicin. For the antagonism assays, capsaicin (30 nM) was included along with increasing concentrations of the test compound. The cells were incubated for 5 min in a water bath at 37 °C. Immediately after incubation, the assay medium was aspirated and the cells were washed twice with DPBS (no Ca^{2+} or Mg^{2+}). The cells were then lysed in radioimmunoprecipitation assay buffer (50 mM Tris-Cl pH 7.5, 150 mM NaCl, 1% Triton X-100, 1% SDS, and 1% sodium deoxycholate; 400 μL/well) for at least 20 min on a shaker. Aliquots (300 μL) of the cell lysates were counted in a liquid scintillation counter. Each data point in the dose response curves for agonism and antagonism represents the mean of the values

from four individual wells. Data from the dose response curves were analyzed by computer fit to the Hill equation. Reported values are the mean of at least three independent experiments unless otherwise indicated. For antagonism measurements, K_i values were calculated from the measured ID_{50} values using the Cheng-Prusoff equation.[13]

4.2.2. MOR binding assay[11,12]

Five μg of protein (5 μL) per assay was incubated in a final volume of 200 μL with 0.9472 nM (K_d) of [^{3}H] DAMGO and unlabeled target material (10^{-5}~10^{-12} M) at 35 °C for 60 min. Total binding was measured in the presence of radioligand and the non-specific binding was determined in the presence of 1 μM unlabeled naloxone. The reaction was terminated by rapid filtration under vacuum using FC96 filter plates (Millipore), followed by washing three times with 200 μL ice-cold 50 mM Tris-HCl (pH 7.4) buffer. The radioactivity of the dried filters was detected in Scint-Axf (Packard) scintillation cocktail with Tri-Carb 2900TR liquid scintillation counter (PerkinElmer). Radioligand binding assays were performed in triplicate. Experimental data were analyzed by GraphPad Prism 5.0 to determine the concentration of the target material that displaced 50% of [^{3}H] DAMGO (IC_{50}). K_i was calculated using the Cheng-Prusoff equation.[13]

4.2.3. Formalin test

ICR male mice weighting 20-25 g in groups of 6-8 were used in all experiments. Male ICR mice were maintained on a 12 h light-dark cycle (light on between 7:00 p.m. and 7:00 a.m.) and allowed free access to food and water. The temperature and humidity of the animal room were maintained at 22 ± 2 ^{o}C and 50 ± 5%, respectively.

The formalin induced licking paw test was modified from the method described by Dubuisson and Dennis.[17] Each mouse was acclimated to an acrylic observation chamber for at least 5 min before the injection of formalin. 20 μL of a 2% solution of formalin in 0.9% saline was injected into the

dorsal surface of the right hindpaw. Each mouse was then placed in an individual clear plastic observational chamber (15 x 15 x 15 cm) and the pain response was recorded for a period of 30 min. The summation of time (in seconds) spent in licking and biting responses of the injected paw during each 5 min block was measured as an indicator of pain response. The test compound was administered intraperitoneally 30 min before formalin injection. The first period (early phase) was recorded 0-5 min after the injection of formalin and the second period (late phase) was recorded 20-30 min after the injection.

4.2.4. Target engagement study

ICR male mice weighting 20-25 in groups of 3-4 were used in all experiments. ICR mice were maintained on a 12 hr light-dark cycle (light on between 7:00 p.m. and 7:00 a.m.) and allowed free access to food and water. The temperature and humidity of the animal room were maintained at 22±2C and 50±5%, respectively. In this study, we followed the national guidelines in conducting animal experiments. All procedures for animal tests were approved by the Medifron Animal Care and Use Committee (approval number, Medifron 2019-4, IACUC). Efforts were made to minimize animal suffering and to reduced the number of animals used.

4.2.4.1. Involvement of the TRPV1 receptor

The involvement of TRPV1 in the antinociceptive activity by **49** was investigated by using the capsaicin-induced paw licking model. Mice were pretreated with **49** or vehicle 30 min prior to injection of 10 μl of capsaicin (3 μg/paw) intraplantarly into the surface of the right hind paw of the mice. The animals were observed individually for 5 min after capsaicin injection. The amount of time spent licking the injected paw was recorded and was considered as an indication of pain behavior.

4.2.4.2. Involvement of the Opioid receptors

To investigate the possible involvement of the opioid system in the antinociceptive activity of **49**, the mice were pre-treated with the mu opioid receptor antagonist, naloxone (10 mg/kg, i.p.) 15 min prior to the administration of **49** or vehicle. After 30 min, the mice were subjected to the formalin-induced paw licking test.

Acknowledgments

This research was supported by the Midcareer Researcher Program (NRF-2019R1A2C2006837) funded by the National Research Foundation of Korea (NRF) and by the Intramural Research Program of the National Institutes of Health, Center for Cancer Research, National Cancer Institute (Project Z1A BC 005270).

References and notes

[1] M-H. Pang, Y. Kim, K.W. Jung, S. Cho, D.H. Lee, A series of case studies: practical methodology for identifying antinociceptive multi-target drugs, Drug Discov. Today 17 (2012) 425-434.

[2] M. Waldhoer, S.E. Bartlett, J.L. Whistler, Opioid receptors, Annu. Rev. Biochem. 73 (2004) 953-990.

[3] A. Szallasi, P.M. Blumberg, Vanilloid (capsaicin) receptors and mechanisms, Pharmacol. Rev. 51 (1999) 159-211.

[4] M.A. Tabrizi, P.G. Baraldi, S. Baraldi, S. Gessi, S. Merighi, P. A. Borea, Medicinal chemistry, pharmacology, and clinical implications of TRPV1 receptor antagonists, Med. Res. Rev. 37 (2017) 936-983.

[5] M.S. Kim, H. Ryu, D.W. Kang, S-H Cho, S. Seo, Y.S. Park, M-Y. Kim, E.J. Kwak, Y.S. Kim, R.S. Bhondwe, H.S. Kim, S-G. Park, K. Son, S. Choi, I. DeAndrea-Lazarus, L.V. Pearce, P.M. Blumberg, R. Frank, G. Bahrenberg, H. Stockhausen, B.Y. Kögel, K. Schiene, T. Christoph, J. Lee,

2‐(3-Fluoro-4-methylsulfonylaminophenyl)propanamides as potent transient receptor potential vanilloid 1 (TRPV1) antagonists: Structure−activity relationships of 2-amino derivatives in the N−(6-trifluoromethylpyridin-3-ylmethyl) C-Region, J. Med. Chem. 55 (2012) 8392-8408.

[6] R. Solimini, S. Pichini, R. Pacifici, F.P. Busardo, R. Giorgetti, Pharmacotoxicology of non-fentanyl derived new synthetic opioids, Front. Pharmacol. 9 (2018) article 654.

[7] J. Ann, W. Sun, X. Zhou, A. Jung, J. Baek, S. Lee, C. Kim, S. Yoon, S. Hong, S. Choi, N.A. Turcios, B.K.A. Herold, T.E. Esch, N.E. Lewin, A. Abramovitz, L.V. Pearce, P.M. Blumberg, J. Lee, Discovery of N-(3-fluoro-4-methylsulfonamidomethylphenyl)urea as a potent TRPV1 antagonistic template, Bioorg. Med. Chem. Lett. 26 (2016) 3603-3607.

[8] S.A. Thorat, A. Jung, J. Ann, S. Y. Ahn, J. Baek, H. Lee, J.M. Kang, C.H. Lee, S. Lee, P.M. Blumberg, D. Kim, E. Kim, K. Son, S. Choi, J. Lee, Structural insight into transient receptor potential vanilloid 1 (TRPV1) agonism and antagonism through 2-oxoquinoline and 1-oxoisoquinoline Urea scaffold, *submitted*.

[9] W. Sun, H-S. Kim, S. Lee, A. Jung, S-E Kim, J. Ann, S. Yoon, S. Choi, J.H. Lee, P.M. Blumberg, R. Frank-Foltyn, G. Bahrenberg, K. Schiene, H. Stockhausen, T. Christoph, S. Frormann, J. Lee, 6,6-Fused heterocyclic ureas as highly potent TRPV1 antagonists, Bioorg. Med. Chem. Lett. 25 (2015) 803-806.

[10] L.V. Pearce, J. Ann, A. Jung, S.A. Thorat, B.K.A. Herold, A.D. Habtemichael, P.M. Blumberg, J. Lee, Novel radiolabeled vanilloid with enhanced specificity for human transient receptor potential vanilloid 1 (TRPV1), J. Med. Chem. 60 (2017) 8246-8252.

[11] D.A. Volpe, G.A. McMahon Tobin, R.D. Mellon, A.G. Katki, R.J. Parker, T. Colatsky, T.J. Kropp, S.L. Verbois, Uniform assessment and ranking of opioid Mu receptor binding constants for selected opioid drugs, Regul. Toxicol. Pharm. 59 (2011) 385-390.

[12] F. Zdor, F. Otvos, S. Benyhe, A. Zimmer, E. Paldy, Inhibition of forebrain l-opioid receptor signaling by low concentrations of rimonabant does not require cannabinoid receptors and directly involves l-opioid receptors, Neurochem. Int. 61 (2012) 378-388.

[13] Y-C. Cheng, W.H. Prusoff, Relationship between the inhibition constant (K_i) and the concentration of inhibitor which causes 50 percent inhibition (I_{50}) of an enzymatic reaction, Biochem. Pharm. 22 (1973) 3099-3108.

[14] M. E. McDonnell, S-P Zhang, N. Nasser, A. E. Dubin, S. L. Dax, 7-Hydroxynaphthalen-1-yl urea and –amide antagonists of human vanilloid receptor 1, Bioorg. Med. Chem. Lett. 14 (2004) 531-534.

[15] K. Urbahns, T. Yura, J.B. Gupta, M. Tajimi, H. Fujishima, T. Masuda, N. Yamamoto, Y. Ikegami, M. Marumo, K. Yasoshima, N. Yoshida, T. Moriwaki, D. Madge, F. Chan, M. Mogi, Tetrahydro-naphthols as orally available TRPV1 inhibitors, Bioorg. Med. Chem. Lett. 22 (2012) 3408-3411.

[16] A. Tjølsen, O.G. Berge, S. Hunskaar, J.H. Rosland, K. Hole, The formalin test: an evaluation of the method, Pain 51 (1992) 5-17.

[17] D. Dubuisson, S.G. Dennis, The formalin test: a quantitative study of the analgesic effects of morphine, meperidine, and brain stem stimulation in rats and cats, Pain 4 (1977) 161-174.

[18] C.P. Ping, T.A.S.T. Mohamad, M.N. Akhtar, E.K. Perimal, A. Akira, D.A.I. Ali, M.R. Sulaiman, Antinociceptive effects of cardamonin in mice: Possible involvement of TRPV1, glutamate, and opioid receptors, Molecules 23 (2018) 2237.

[19] Z-Y. Yin, L. Li, S-S. Chu, Q. Sun, Z-L. Ma, X-P. Gu, Antinociceptive effects of dehydrocorydaline in mouse models of inflammatory pain involve the opioid receptor and inflammatory cytokines, Sci. Rep. 6 (2016) 27129.

- A series of dual-acting ligands were investigated for novel analgesic agents.
- Compound **49** displayed promising dual-acting activity toward TRPV1 and MOR.
- Compound **49** showed potent and dose-dependent antinociceptive activity in formalin assay.